PERGAMON

International Journal of Plasticity 18 (2002) 531–547

INTERNATIONAL JOURNAL OF Plasticity

www.elsevier.com/locate/ijplas

Constitutive relations for cohesionless frictional granular materials

Sia Nemat-Nasser* and Juhua Zhang

Center of Excellence for Advanced Materials, Department of Mechanical and Aerospace Engineering, University of California, San Diego, La Jolla, CA 92093-0416, USA

Received in final revised form 1 February 2001

Dedicated to Thomas Wright on his 65th birthday

Abstract

Based on the micro-mechanical model recently developed by Nemat-Nasser S. (J. Mech. Phys. Solids 48 (2000) 1541), a three-dimensional continuum mechanics model is presented for the deformation of granular materials which carry the applied load through frictional contacts. The model incorporates the anisotropy (or fabric) which develops as a frictional granular mass is deformed in shear, and includes the coupling between shearing and volumetric straining (or dilatancy). The model parameters are estimated, based on the results of a series of cyclic shearing experiments on large hollow cylindrical samples of silica sand. Then, the model is used to predict other experimental results, arriving at good correlation.

Keywords: Coustitutive models; Granular materials; Cyclic streaming; Coulomt friction; Anisotropy; Fabric

1. Introduction

In a recent article, Nemat-Nasser (2000) presents a two-dimensional model to describe the deformation of granular masses which carry the applied load through frictional contact. The model incorporates the experimentally observed response of two-dimensional photo-elastic frictional rods of oval cross-section, deformed under biaxial and simple shearing (Oda et al., 1982; Subhash et al., 1991). In this formulation, the anisotropy or fabric is represented by the distribution of the contact

* Corresponding author. Tel.: +1-858-534-2727; fax: +1-858-534-2727.
E-mail address: ceam@ames.ucsd.edu (S. Nemat-Nasser).

0749-6419/02/$ - see front matter
PII: S0749-6419(01)00008-0

unit normals and this distribution is represented by a deviatoric second-order tensor. Directly calculating the resistance to sliding due to isotropic Coulomb friction, as well as that due to the anisotropic distribution of contact normals, Nemat-Nasser shows that the stress tensor, $\boldsymbol{\tau}$, can be represented by the sum of a pressure, $p\mathbf{1}$, a deviatoric backstress which is proportional to the fabric tensor, $\boldsymbol{\beta}$, and a deviatoric tensor, $\mathbf{S}$, representing the internal isotropic resistance to deformation, arriving at

$$\boldsymbol{\tau} = \mathbf{S} - p\mathbf{1} + \boldsymbol{\beta} \tag{1}$$

or, using a rectangular Cartesian coordinate system,

$$\tau_{ij} = S_{ij} - p\delta_{ij} + \beta_{ij}, \quad i,j = 1,2,3. \tag{2}$$

Here, $\mathbf{1}$ with components δ_{ij} is the identity tensor, $p = -\frac{1}{3}\tau_{kk} = -\frac{1}{3}tr\boldsymbol{\tau}$ is the pressure, and $tr\mathbf{S} = tr\boldsymbol{\beta} = 0$. The backstress $\boldsymbol{\beta}$, is proportional to the pressure p, and an effective friction coefficient. Its magnitude, defined by the quantity $\beta = (\frac{1}{2}\boldsymbol{\beta} : \boldsymbol{\beta})^{\frac{1}{2}}$, gives the degree of anisotropy, and the orientation of its principal axes defines the orientation of the anisotropy axes at each material point of the corresponding continuum model. These axes are situated along the directions of the extrema of the density of the unit contact normal vectors, i.e. the principal axes of the fabric tensor of the actual granular mass. It is, therefore, assumed that each material neighborhood of the continuum model, is endowed with the average properties of a uniform sample of the actual granular materials, consisting of a large number of granules. The deviatoric stress tensor $\mathbf{S}$ with components S_{ij}, and effective value (magnitude) $\tau = (\frac{1}{2}\mathbf{S} : \mathbf{S})^{\frac{1}{2}}$, represents the isotropic resistance of the granular material. It will be called the stress difference. It is assumed that the magnitude of $\mathbf{S}$ is given by $\tau = p\sin\phi_\mu$, where ϕ_μ is an effective isotropic friction coefficient. Generalizing the double sliding models (Spencer, 1964, 1982, 1986; De Josselin de Jong, 1971;Mehrabadi and Cowin, 1978; Balendran and Nemat-Nasser, 1993a, b), Nemat-Nasser (2000) shows that the inelastic deformation rate tensor, $\mathbf{D}^p$, for the two-dimensional case can be represented by

$$\mathbf{D}^p = \dot{\gamma}\frac{\boldsymbol{\mu}}{\sqrt{2}} + \hat{\alpha}\left(\mathbf{1}^{(4s)} - \boldsymbol{\mu}\otimes\boldsymbol{\mu}\right) : \mathbf{D}' + \frac{1}{2}\dot{\gamma}B\mathbf{1} \tag{3}$$

or, in component form, by

$$D^p_{ij} = \dot{\gamma}\frac{\mu_{ij}}{\sqrt{2}} + \hat{\alpha}\left(1^{(4s)}_{ijkl} - \mu_{ij}\mu_{kl}\right)D'_{kl} + \frac{1}{2}\dot{\gamma}B\delta_{ij}, \tag{4}$$

where $\mathbf{1}^{(4s)}$ with components $1^{(4s)}_{ijkl} = \frac{1}{2}\left(\delta_{ik}\delta_{jl} + \delta_{il}\delta_{jk}\right)$ is the fourth-order symmetric unit tensor; $\hat{a}$ is a noncoaxiality coefficient; $\mathbf{D}'$ is the deviatoric part of the deformation rate tensor; $\dot{\gamma}$ is an effective inelastic deformation rate; and B is the dilatancy parameter. If the continuum velocity field is given by $\mathbf{v} = \mathbf{v}(\mathbf{x}, t)$, then the deformation rate is the symmetric part of $\frac{\partial\mathbf{v}}{\partial\mathbf{x}}$ of components $\frac{\partial v_i}{\partial x_j}$, and $\mathbf{D}^p$ is the corresponding plastic part. In Eq. (3), the second-order unit tensor $\boldsymbol{\mu}$ is defined by

$$\boldsymbol{\mu} = \frac{\mathbf{S}}{\sqrt{2\tau}}, \boldsymbol{\mu} : \boldsymbol{\mu} = 1. \tag{5}$$

In the present work, we will generalize the micro-mechanically based model of Nemat-Nasser (2000) into a fully three-dimensional case and relate it to the more classically-based frictional models (Rudnicki and Rice, 1975; and Nemat-Nasser and Shokooh, 1980). The present paper is organized, as follows. In Section 2, the general three-dimensional continuum model is presented and its results are related to the corresponding micro-mechanical counterparts. The basic equations are valid for large elastoplastic deformation of granular materials under general shearing and compression. In particular, a general relation among the parameters which define dilatancy, pressure sensitivity, and fabric anisotropy, is established, using an energy approach (Nemat-Nasser, 1980; Nemat-Nasser and Shokooh, 1980). The experimental results of cyclic torsional tests on a silica sand performed using special large hollow cylindrical samples (Okada, 1992; Okada and Nemat-Nasser, 1994) are summarized in Section 3.Using these experimental results, constitutive parameters defining the evolution of the fabric and the void ratio are presented in Section 4, and the theoretical and experimental results are compared. Several conclusions are summarized in Section 5.

2. General equations

To generalize the model defined by (3), for application to possibly large deformations, consider the following yield surface and flow potential:

$$f \equiv \tau - F(I, \Delta, \gamma), \tag{6}$$

$$g \equiv \tau + G(I, \Delta, \gamma), \tag{7}$$

where

$$\Delta = \int_0^t \frac{\rho_0}{\rho} D^p_{kk} \mathrm{d}t, \tag{8}$$

$$\gamma = \int_0^t \dot{\gamma} \mathrm{d}t, \tag{9}$$

$$\tau = \left\{ \frac{1}{2} (\boldsymbol{\tau}' - \boldsymbol{\beta}) : (\boldsymbol{\tau}' - \boldsymbol{\beta}) \right\}^{\frac{1}{2}}, \tag{10}$$

$$I = \tau_{kk} = -3p. \tag{11}$$

Here, again, $\boldsymbol{\beta}$ is the backstress; $\boldsymbol{\tau}' = \boldsymbol{\tau} + p\mathbf{1}$ is the deviatoric part of the total stress $\boldsymbol{\tau}$; $\dot{\gamma}$ is the effective inelastic deformation rate; Δ is the total accumulated

plastic volumetric strain, measured relative to a reference state with mass density ρ_0, the current mass density being ρ; and p is the pressure. For finite inelastic deformations, it is necessary to measure deformations from some reference state. For small strains, Δ is the volumetric plastic strain, usually denoted by ϵ^p_{kk}. Based on (3), the plastic deformation rate tensor is defined by

$$\begin{aligned}\mathbf{D}^p &= \dot\gamma\frac{\partial g}{\partial\boldsymbol\tau} + \eta\hat\alpha\big(\mathbf{1}^{(4s)} - \boldsymbol\mu\otimes\boldsymbol\mu\big) : \mathbf{D}' \\ &= \dot\gamma\frac{\boldsymbol\mu}{\sqrt{2}} + \eta\hat\alpha\big(\mathbf{1}^{(4s)} - \boldsymbol\mu\otimes\boldsymbol\mu\big) : \mathbf{D}' + \frac{1}{3}\dot\gamma B\mathbf{1}.\end{aligned} \tag{12}$$

$$B = -\frac{\partial G}{\partial p}, \tag{13}$$

where $\hat\alpha \geqslant 0$ is the noncoaxiality coefficient; and $\eta = \pm 1$ denotes the direction of the noncoaxial plastic deformation rate relative to the yield surface, chosen such that the corresponding rate of plastic work is nonnegative. In (12), the dilatancy parameter, B, relates the shear-induced volumetric strain rate to the shear strain rate. The unit tensor $\boldsymbol\mu$, coaxial with the stress difference $\mathbf{S} = \boldsymbol\tau' - \boldsymbol\beta$, is defined in (5).

To complete the model, it is necessary to define a rule for the variation of the backstress with deformation. We assume that the Jaumann rate of change of the backstress $\boldsymbol\beta$ is given by

$$\mathring{\boldsymbol\beta} = \sqrt{2}p\Lambda\dot\gamma\boldsymbol\mu, \tag{14}$$

where Λ is a material function (see Section 4). This assumption is based on the experimental observation that the fabric tensor tends to become coaxial with the stress tensor (Oda et al., 1982; Subhash et al., 1991). In (14) the Jaumann rate of change of the second-order symmetric tensor $\boldsymbol\beta$ is defined by

$$\mathring{\boldsymbol\beta} = \dot{\boldsymbol\beta} - \mathbf{W}\boldsymbol\beta + \boldsymbol\beta\mathbf{W} \tag{15}$$

or in component

$$\mathring\beta_{ij} = \dot\beta_{ij} - W_{ik}\beta_{kj} + \beta_{ik}W_{kj}, \tag{16}$$

where $\mathbf{W}$ is spin tensor, i.e. the antisymmetric part of the velocity gradient $\dfrac{\partial\mathbf{v}}{\partial\mathbf{x}}$.

For continued plastic flow, $\dot f = 0$. This yields

$$\dot\gamma = \frac{1}{\bar H}\left\{\frac{\boldsymbol\mu}{\sqrt{2}} + \frac{M}{3}\mathbf{1}\right\} : \mathring{\boldsymbol\tau}, \tag{17}$$

$$M = \frac{\partial F}{\partial p}, \tag{18}$$

$$\bar{H} = \frac{\rho_0}{\rho} B \frac{\partial F}{\partial \Delta} + \frac{\partial F}{\partial \gamma} + \frac{\boldsymbol{\mu} : \overset{\circ}{\boldsymbol{\beta}}}{\sqrt{2}\dot{\gamma}} = \frac{\rho_0}{\rho} B \frac{\partial F}{\partial \Delta} + \frac{\partial F}{\partial \gamma} + p\Lambda. \tag{19}$$

The orientation of the fabric tensor is defined by the following unit tensor:

$$\boldsymbol{\mu}_\beta = \frac{\boldsymbol{\beta}}{\sqrt{2}\beta}, \quad \beta = \left(\frac{1}{2}\boldsymbol{\beta} : \boldsymbol{\beta}\right)^{\frac{1}{2}}. \tag{20}$$

The elastic response of a granular mass also depends on the fabric, and, in general, is anisotropic. It is reasonable to expect that the principal directions of the fabric tensor also define the elastic anisotropy axes, since the former axes correspond to the extrema of the density of contact normals. Then following Nemat–Nasser (2000), it can be shown that the fourth-order elasticity tensor is given by

$$\boldsymbol{\mathcal{L}} = 2\mu\left(\mathbf{1}^{(4s)} - \frac{1}{3}\mathbf{1}\otimes\mathbf{1}\right) + 2\bar{\mu}\boldsymbol{\mu}_\beta \otimes \boldsymbol{\mu}_\beta + \frac{1}{2}\bar{K}\left(\boldsymbol{\mu}_\beta \otimes \mathbf{1} + \mathbf{1}\otimes\boldsymbol{\mu}_\beta\right) + \frac{1}{9}K\mathbf{1}\otimes\mathbf{1}, \tag{21}$$

with components

$$L_{ijkl} = 2\mu\left(1^{(4s)}_{ijkl} - \frac{1}{3}\delta_{ij}\delta_{kl}\right) + 2\bar{\mu}\mu_{\beta ij}\mu_{\beta kl} + \frac{1}{2}\left(\eta_{\beta ij}\delta_{kl} + \delta_{ij}\mu_{\beta kl}\right) + \frac{1}{9}K\delta_{ij}\delta_{kl}, \tag{22}$$

where μ, $\bar{\mu}$, K, and $\bar{K}$ are the elastic moduli. The final constitutive relation is now expressed by

$$\overset{\circ}{\boldsymbol{\tau}} = \boldsymbol{\mathcal{L}} : (\mathbf{D} - \mathbf{D}^p), \tag{23}$$

where $\mathbf{D}$ is the deformation rate tensor, $\mathbf{D}^p$ is defined by (12), and $\overset{\circ}{\boldsymbol{\tau}}$ is the Jaumann rate of change of $\boldsymbol{\tau}$. Substituting (12), (21), and (23) into (17), one obtains

$$\begin{aligned}
\dot{\gamma} &= \frac{A_1 + A_2}{\bar{H} + \mu + \bar{\mu}\mu_\beta^2 + \dfrac{\mu_\beta}{2\sqrt{2}}(B+M)\bar{K} + \dfrac{1}{9}MKB}, \\
A_1 &= \sqrt{2}\left(\mu D_\mu + \bar{\mu}\mu_\beta D_\beta\right) + \left(\frac{\bar{K}\mu_\beta}{2\sqrt{2}} + \frac{MK}{9}\right)D_{kk} + \frac{1}{2}M\bar{K}D_\beta, \\
A_2 &= \left(\sqrt{2}\eta\hat{\alpha}\bar{\mu}\mu_\beta + \frac{1}{2}M\bar{K}\eta\hat{\alpha}\right)\left(\mu_\beta D_\mu - D_\beta\right),
\end{aligned} \tag{24}$$

where, $D_\mu = \mathbf{D} : \boldsymbol{\mu}$, $\mu_\beta = \boldsymbol{\mu}_\beta : \boldsymbol{\mu}$, and $D_\beta = \mathbf{D} : \boldsymbol{\mu}_\beta$.

The rate of plastic work is given by

$$\dot{w}_{pd} = \left(\boldsymbol{\beta} + \sqrt{2}\tau\boldsymbol{\mu}\right) : \frac{1}{\sqrt{2}}\dot{\gamma}\boldsymbol{\mu} - p\dot{\gamma}B = \left(\frac{\tau}{p} + \frac{1}{\sqrt{2}p}\boldsymbol{\beta} : \boldsymbol{\mu} - B\right)p\dot{\gamma}. \tag{25}$$

The rate of frictional loss, $\dot{w}_f$, due to internal sliding and rolling of the granules is approximated by

$$\dot{w}_{\mathrm{f}} = \tau_{\mathrm{f}}\dot{\gamma} = pM_{\mathrm{f}}\dot{\gamma} \tag{26}$$

where M_{f} is an effective overall frictional coefficient. This assumption generalizes the usual frictional energy loss which is proportional to the applied pressure and the rate of sliding $\dot{\gamma}$, the proportionality coefficient, M_{f}, being the friction coefficient. By setting the rate of frictional loss equal to the rate of plastic work, a relation among parameters relating to dilatancy, fabric, and friction is obtained (Nemat-Nasser, 2000),

$$B = -M_{\mathrm{f}} + \frac{\tau}{p} + \mu_{\mathrm{f}}, \tag{27}$$

$$\mu_{\mathrm{f}} = \frac{1}{\sqrt{2}p}\boldsymbol{\beta} : \boldsymbol{\mu}. \tag{28}$$

Since $M_{\mathrm{f}} > 0$, Eq. (27) shows that the initial plastic shearing of an initially isotropic sample of frictional granular materials, is generally accompanied by densification. For sands under small confining pressures, this is generally observed (Okada and Nemat-Nasser, 1994).

For small pressures, it may be assumed that the solid particles are rigid. In that case, the plastic volumetric deformation rate relates to the void ratio, e, which is the volume of voids divided by the volume of solid, by

$$D^p_{kk} = B\dot{\gamma} = \frac{\dot{e}}{1+e} \tag{29}$$

which, upon integration, yields

$$e = (1+e_0)\exp\left(\int_0^{\gamma} B\,d\gamma\right) - 1, \tag{30}$$

where e_0 is the initial void ratio.

3. Experimental results

In this section, we review the results of cyclic torsional tests performed on sand under drained conditions using a hollow cylindrical apparatus (Okada, 1992). The schematic diagram of the hollow cylindrical sample is given in Fig. 1a, and the stress state in a sample element is shown in Fig. 1b. The sample consists of a hollow cylindrical mass of granular materials with 20 cm inside diameter, 25 cm outside diameter, and 25 cm height. It is subjected to a uniform confining pressure (axially,

internally, and externally), and then sheared in torsion. In the experiment, first the specimen is isotropically consolidated under an effective pressure of 196 kPa. Upon completion of the consolidation, the specimen is subjected to a strain-controlled cyclic torsional shearing while the normal stresses are kept constant. Consider the polar coordinates as shown in Fig. 1a. The state of stress in a shell element of the sample is then such that $\tau_{rr} = \tau_{\theta\theta} = \tau_{zz} = -p$, and $\tau_{r\theta} = \tau_{rz} = 0$. During the course of deformation, the inner and outer surfaces of the shell are free to move away or towards the center of the cylinder, causing a hoop strain $\varepsilon_{\theta\theta}$ and a radial strain ε_{rr}. The sample is also free to dilate or contract axially, causing an axial strain ε_{zz}. In the experiment, the shear strain $\varepsilon_{\theta z}$ and the confining pressure p are controlled and the shear stress and the axial and volumetric strains are measured. In order to simulate

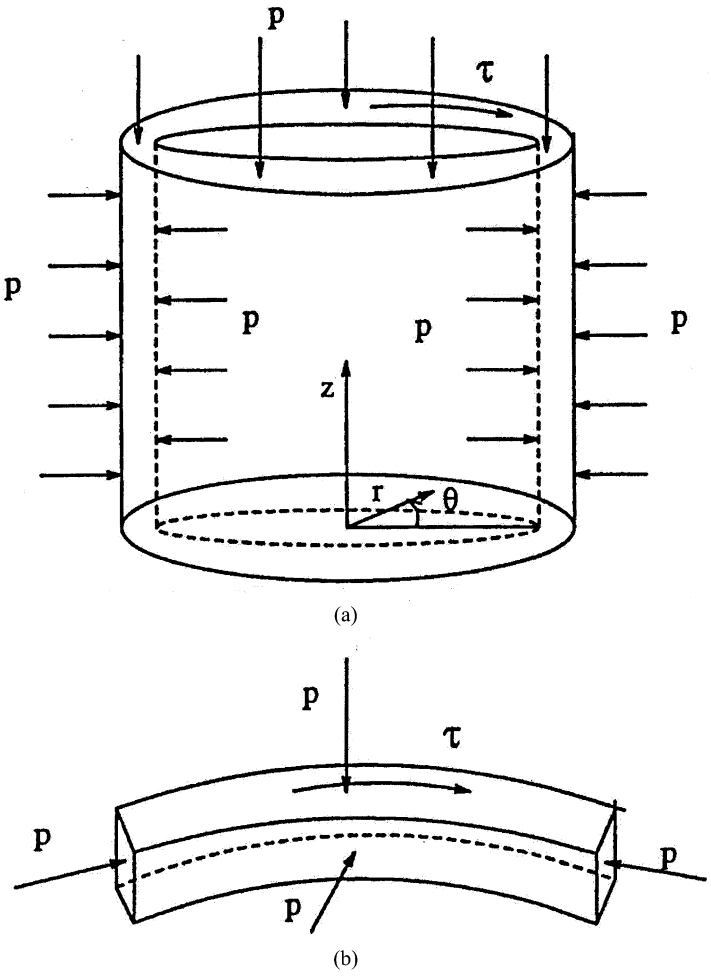

Fig. 1. (a) Schematic diagram of a hollow cylindrical sample subjected to a hydrostatic pressure p and a torsional shear stress τ. (b) State of stress in an element of the hollow cylindrical sample.

the experimental results, we assume that the sample deforms homogeneously along the cylindrical axis. Noting that the thickness (2.5 cm) of the sample is much smaller than its height (25 cm) and its mid-thickness diameter (22.5 cm), we neglect the thickness strain, i.e. we set $\varepsilon_{rr} \approx 0$. As a result, the deformation can be modeled as a simple shearing in the θ,z-plane under constant pressure. We denote the θ-direction by x_1, and the z-direction by x_2.

Shown in Fig. 2a and b are the experimental results of relations between the stress ratio (τ_{12}/p), the void ratio (e), and the shear strain in cyclic shearing of *Silica* 60 sand with an initial void ratio of $e_0 = 0.831$. For *Silica* 60, the minimum and maximum void ratios are $e_m = 0.631$ and $e_M = 1.095$, respectively; as measured by the JSSMFE method (see Committee of JSSMFE on the Test Method of Relative Density of Sand, 1979).

Using the experimental data, we have calculated the variation of the quantity $\frac{\delta\tau_{12}}{p\delta\varepsilon_{12}}$ with respect to the shear strain for the indicated cycles of deformation in Fig. 2a, and have obtained the results presented in Figs. 3a and b. These experimental results reveal that:

1. The elastic range is quite small for this cohesionless sand under the drained condition, in loading, in unloading, and in reloading.
2. The shearing resistance depends on the fabric which in turn changes with the shear strain. The shear-deformation-history dependency for both the loading and unloading paths may be characterized by the shear strain amplitude. Within each shearing cycle, the resistance to shearing increases with increasing straining, attaining its maximum value at the maximum shear amplitude. Upon strain reversal, there is a sudden decrease (jump) in the shear resistance to its minimum value; see Fig. 3a and b.
3. The shear stress–strain path is not very sensitive to changes in the void ratio.
4. On completion of each cycle of shearing deformation, there is a net densification.
5. The amount of net densification per cycle is related to the shear strain amplitude, and it decreases with the number of cycles of constant shear strain amplitude.

It should be noted that the above observations are generally valid for most cohesionless frictional granular materials that are sheared under small confining pressures.

4. Modeling cyclic shear behavior

In this section, we consider the cyclic shearing problem discussed in Section 3, reduce the general constitutive equations presented in Section 2 to this case, and seek to identify the material functions based on the experimental results.

4.1. Relation between shear strain and shear stress

A simple shearing problem is used to represent the experiment. The components of the unit tensor $\boldsymbol{\mu}$, then are

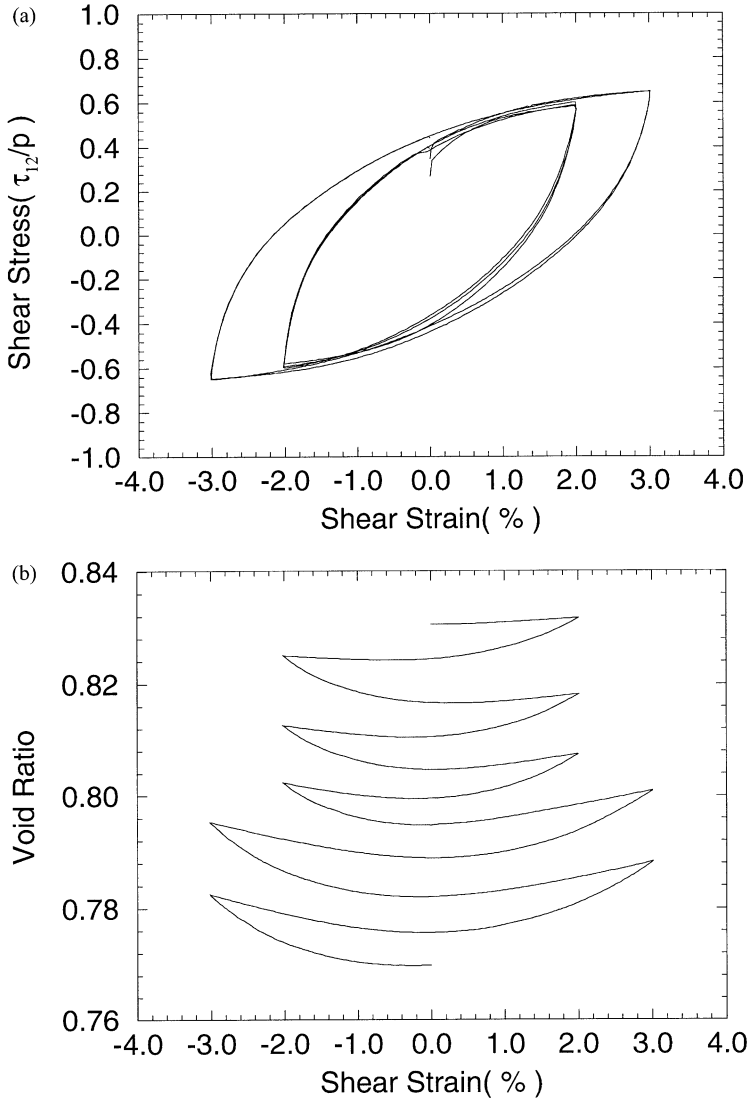

Fig. 2. Experimental result: relation between (a) normalized shear stress and shear strain and (b) void ratio and shear strain.

$$\mu_{ij} = \begin{cases} \pm\dfrac{\sqrt{2}}{2} & \text{if } i=1,\ j=2 \text{ or } j=1,\ i=2 \\ 0 & \text{otherwise} \end{cases} \tag{31}$$

In the sequel, the '+' corresponds to the loading or reverse unloading. In this situation, the stress difference has the same orientation as the back stress, and for simple shearing, the shear strain is an increasing function of time. The '−' means the

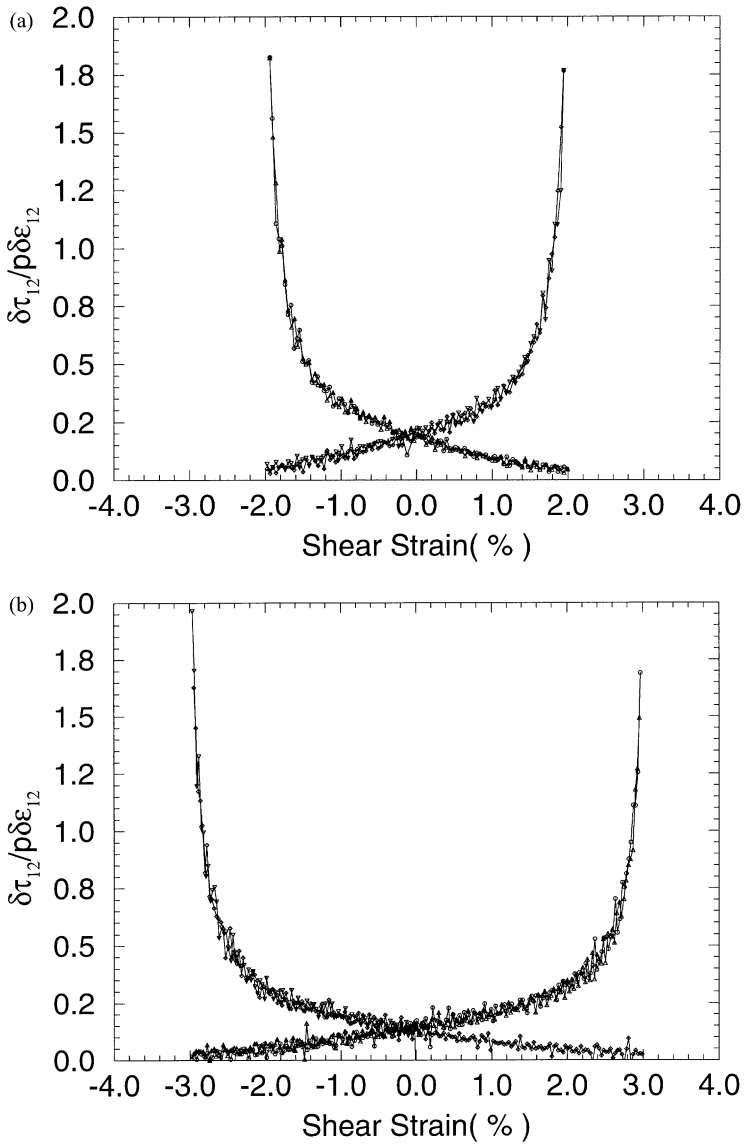

Fig. 3. Rate of change of normalized shear stress with respect to shear strain, vs. shear strain: shear strain amplitude is (a) 2.0%; void ratio changes from 0.83 to 0.80 and (b) 3.0%; void ratio changes from 0.80 to 0.77.

unloading or reverse loading, where the stress difference has an orientation opposite to that of the back stress. Then the shear strain is a decreasing function of time.

Substituting (31) into (14), we obtain

$$\mathring{\beta}_{11} = \mathring{\beta}_{22} = 0. \tag{32}$$

Since the initial state is isotropic, (32) shows that $\beta_{11} = \beta_{22} =$ constant, and in view of (16), we obtain

$$\dot{\beta}_{12} = \sqrt{2}p\Lambda\dot{\gamma}\mu_{12} + W_{12}(\beta_{22} - \beta_{11}) = \pm p\Lambda\dot{\gamma}, \tag{33}$$

and it follows that the spin, W_{12}, has no effect on the back stress in this simple case.

As is seen from (24), the elastic parameters affect the plastic strain rate, $\dot{\gamma}$. For simple shearing, $\boldsymbol{\mu}_\beta = \pm\boldsymbol{\mu}$, $\mu_\beta = \pm 1$, in (24), and $D_\mu\mu_\beta - D_\beta = 0$, so that $A_2 = 0$. When the applied pressure is constant, it is reasonable to assume that the elastic bulk strain rate $D^e_{kk} = D_{kk} - D^p_{kk} \approx 0$. Hence $D_{kk} \approx D^p_{kk} = B\dot{\gamma}$. Now, (24) reduces to

$$\dot{\gamma} = \frac{\sqrt{2}(\mu + \bar{\mu})D_\mu + \dfrac{1}{2}M\bar{K}D_\beta}{\bar{H} + \mu + \bar{\mu} + \dfrac{1}{2\sqrt{2}}\mu_\beta\bar{K}M}, \quad D_\mu = \pm\sqrt{2}D_{12}. \tag{34}$$

As mentioned in Section 3, the elastic strains are so small that they can be neglected. For small pressures, the effective stress difference, and hence, the radius of the yield surface $F(I, \Delta, \gamma)$, are also negligibly small. The shear stress rate is, therefore, given by

$$\dot{\tau}_{12} \approx \dot{\beta}_{12} = \pm p\Lambda\dot{\gamma}. \tag{35}$$

Expression (34) defines $\dot{\gamma}$. It involves quantities $\frac{\partial F}{\partial \Delta}$, $\frac{\partial F}{\partial \gamma}$, and $M = \frac{\partial F}{\partial p}$, which generally are very small relative to the elastic shear modulus. We neglect these quantities, and noting that pressure is constant under a drained condition, reduce (34) to

$$\dot{\gamma} = \pm\frac{2D_{12}}{1 + \dfrac{\Lambda}{\kappa}}, \quad \kappa = \frac{\mu + \bar{\mu}}{p}. \tag{36}$$

The shear moduli μ and $\bar{\mu}$, in general depend on the void ratio. As an approximation, we use a linear function to describe the relation between the shear modulus and the void ratio as follows:

$$\kappa = \kappa_0(1 + c(e_{\mathrm{M}} - e)) \tag{37}$$

where c is a material parameter. When the void ratio attains its maximum value, e_{M}, then the elastic moduli are at their minimum value (see, e.g. Nemat-Nasser and Hori, 1993). The maximum values of the moduli correspond to the minimum void ratio, as should be expected.

4.2. Evolution of fabric

The fabric changes with continued plastic deformation of the granular mass. This change must be quantified in terms of the deformation or stress measures.

As frictional granules are sheared under a confining pressure, the distribution of contact normals and contact forces changes, as more contacts are developed in the direction of maximum compression (Nemat-Nasser, 1980; Oda et al., 1982; Subhash et al. 1991). This process leads to greater induced anisotropy, as shearing continues. The microstructure of the granular mass changes such as to increase its resistance to this continued shearing, by increasing the density of the contacts in the direction of the maximum principal compression, while the density of contacts in the direction of the minimum compression decreases. In this process, the stress and the fabric tensors tend to become coaxial and in-phase with each other, i.e. the directions of the maximum compression (principal stress) and the maximum contact density tend to coincide. For cyclic shearing under constant pressure, the maximum induced anisotropy is, therefore, attained at the extreme values of the shear strain.

Upon the reversal of shearing, there is a substantial change in the relative orientation of the stress and the fabric tensors, i.e. they are suddenly out-of-phase with each other. Hence, the resistance due to the fabric, is suddenly reduced to a minimum value, and continues to decrease during the early stages of unloading, as has been shown experimentally and discussed elsewhere (Balendran and Nemat-Nasser, 1993a; Nemat-Nasser, 2000). We therefore conclude that the shear-deformation-history dependency can be represented by the extrema of the shear strain during each cycle of deformation. This quantity has an important influence on the subsequent stress–strain path.

Although the elastic range is quite small and can be neglected for the considered cohesionless sand subjected to cyclic drained shearing under a small pressure, Figs. 3a and b show that the elastic moduli are still important parameters.

Figs. 2a, and 3a and b show that the stress–stain path is almost independent of the void ratio. Figs. 3a and b show that the slope of the shear stress (normalized with respect to pressure) versus the shear strain is symmetric about the zero shear strain. Based on these experimental results, we assume that the fabric evolution coefficient Λ in (14) and (33) has the following form:

$$\Lambda = \frac{\kappa}{1 + a|\varepsilon - \varepsilon^e|^n}, \tag{38}$$

where a and n are constants to be determined empirically from experiments. In (38) $\varepsilon = \varepsilon(t) = \int_0^t D_{12}\mathrm{d}t$, and ε^e is the value of $\varepsilon(t)$, attained just before the shearing is reversed.

The stress–strain path is now obtained by integrating (35)–(38). The comparison between the model prediction and the experimental results is shown in Figs. 4a and b. The required material parameters are listed in Table 1. The dashed lines represent the experimental data, and the solid lines correspond to the model results. Here, ε^e, has values ± 0.02 and ± 0.03, respectively. The effective pressure in the experiments was $p = 1.96 \times 10^5$ Pa.

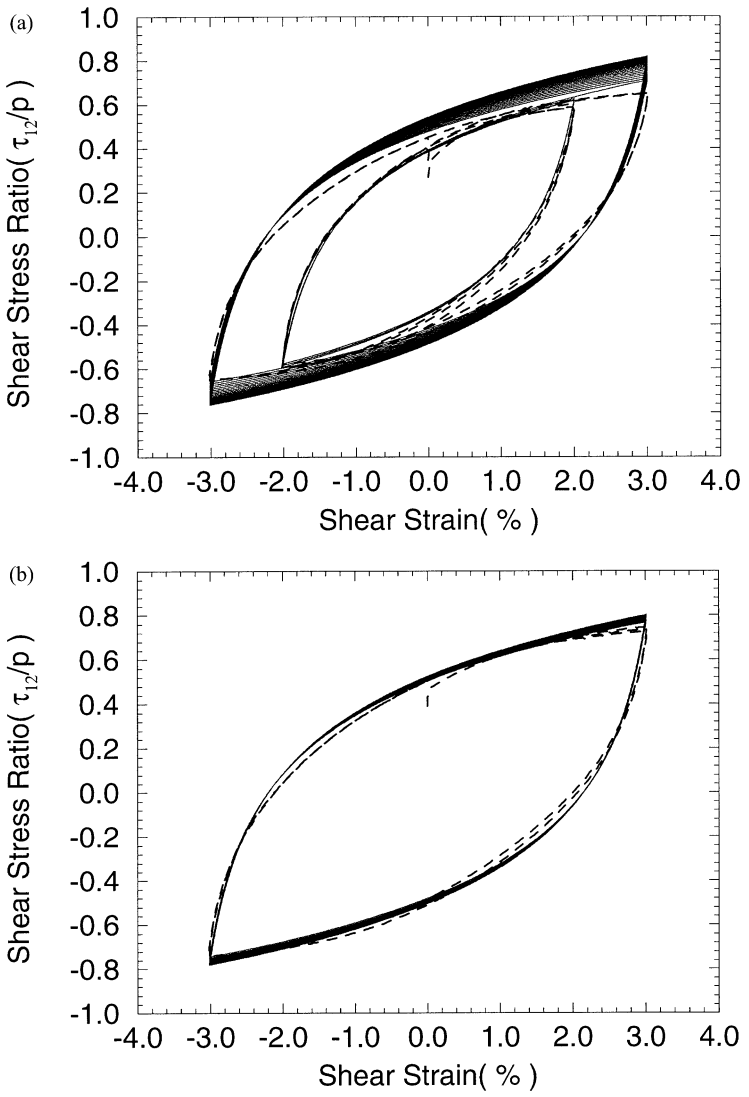

Fig. 4. Relation between normalized shear stress and shear strain in multi-cycle shearing: solid lines — model prediction; dashed lines — experimental results. The void ratio of the virgin sample is: (a) 0.867 and (b) 0.719, respectively.

4.3. Dilatancy and friction

A very small elastic range means that the radius of the yield surface is negligibly small. In addition, while the dilatancy Eq. (27) is a direct consequence of the energy balance, expression (26) is an approximation, and, therefore may have to be adjusted. The authors have found that, for the present simple problem, (27) must be rewritten as

Table 1
The parameters used in the model

κ_0	c	a	n	d	b	n_1	n_2	ζ
130.0	1.42	1.40×10^3	1.1	0.25	0.10	0.40	1.0	0.75

$$B = M_f + \zeta\mu_f, \quad \mu_f = \pm\frac{\beta_{12}}{p}, \tag{39}$$

where $\zeta \leqslant 1$ is a parameter to be determined empirically. In view of (29), (35), and (39), we obtain

$$B = \pm\frac{p\Lambda}{1+e}\frac{de}{d\tau_{12}}, \quad M_f = B + \zeta\mu_f. \tag{40}$$

The quantity $\frac{de}{d\tau_{12}}$ can be obtained from the experimental data, and Λ can be calculated from (38), so that M_f can be calculated from (40). Fig. 5 shows how the overall friction coefficient M_f changes with the shear strain.

It is clear that the overall friction coefficient depends on the fabric. When the shear strain increases from a minimum value to a maximum value, or when it decreases from a maximum value to a minimum value, the fabric, characterized by the value of μ_f, changes monotonically from a minimum value to a maximum value. This suggests that the value of μ_f suffers a jump from a maximum value to a minimum value upon the strain reversal at the extreme values of the shear strain, in a cyclic shearing. It is reasonable to assume that the overall friction resistance increases monotonically

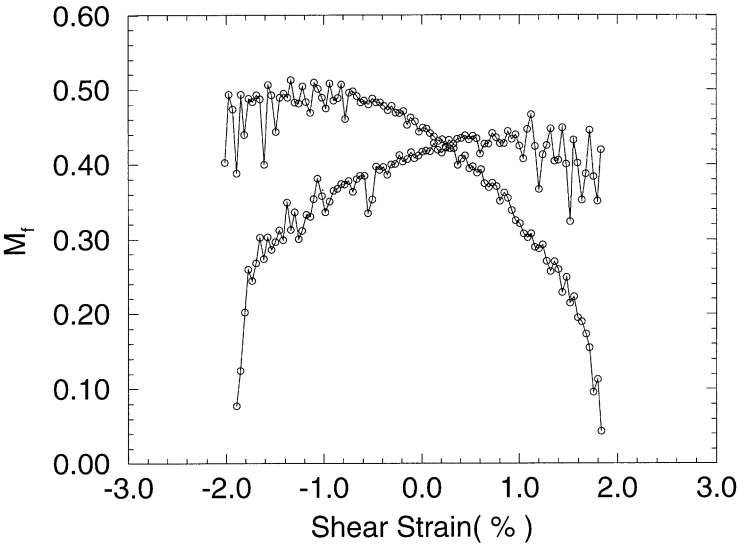

Fig. 5. Relation between overall friction coefficient and shear strain.

with increasing μ_f. Upon strain reversal at the extreme values of the shear strain, the response is elastic at the beginning of unloading, even if the elastic range is assumed to be very small. When the value of the fabric parameter μ_f jumps from a maximum to a minimum value, the value of the overall friction coefficient in the dilatancy Eq. (27) also suddenly changes from a maximum value to zero at the strain reversal points. In addition to its dependence on the fabric, the friction coefficient also depends on the void ratio. Experimental results (Okada, 1992) show that in each

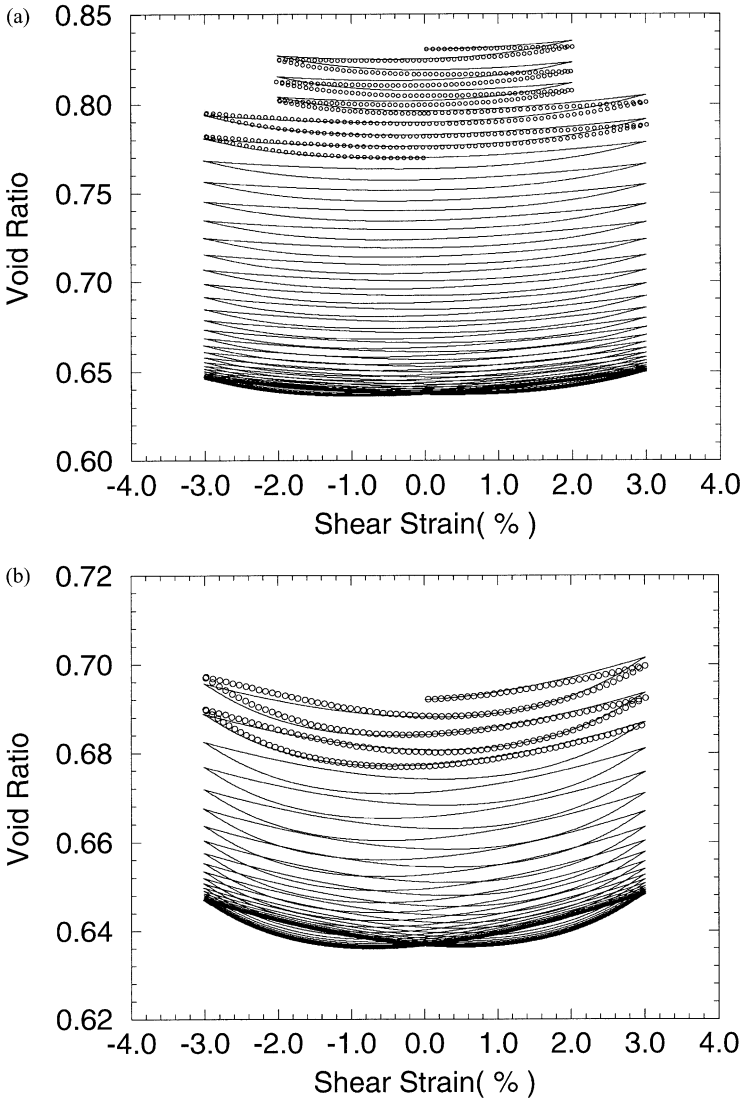

Fig. 6. Relation between void ratio and shear strain in multi-cycle shearing: solid lines — model prediction; circles — experimental data. The void ratio of the virgin sample is: (a) 0.867; (b) 0.719, respectively.

cycle of shearing deformation, there is a net densification, and this net densification per cycle decreases with the number of cycles. In view of (30) and (39), it follows that, as the void ratio decreases, the quantity M_f decreases. In view of these observations, we consider the following model for the overall friction coefficient:

$$M_f = (d + b(e - e_m)^{n_1})(\mu_0 + \mu_f)^{n_2}, \tag{41}$$

where e_m is the minimum void ratio; μ_0 is the reference value of the fabric parameter μ_f, within each cycle; and d, b, n_1, and n_2 are material parameters. At the beginning of loading of a virgin sample, if the void ratio is near its maximum value e_M, then the reference value μ_0 must be large to ensure densification ($e \leqslant e_M$), and if the void ratio is near its minimum value e_m, then μ_0 must be very small, nearly zero, so that there is dilatancy ($e \geqslant e_m$). In the course of cyclic shearing, the value of μ_0 is taken to be the maximum value that the fabric parameter μ_f attains just before unloading. Therefore, the value of μ_0 changes twice during each cycle of shearing.

The comparison between the calculation results and the experimental results is shown in Fig. 6. The required material parameters and their values are listed in Table 1. The circles represent the experimental data, and the solid lines correspond to the model results. As shown in Figs. 6a and b, the model predictions are in reasonable agreement with the experimental results. When work hardening is neglected, the shear stress depends only on the shear strain for the same shear strain amplitude in each shearing cycle. Eq. (41) shows that when the void ratio approaches its minimum value, the overall friction coefficient M_f depends only on the fabric (shear stress). In this case, with the increasing number of shearing cycles, the void ratio converges to a limiting case as shown in Fig. 6.

5. Conclusions

In this work we have presented an elasto-plastic continuum constitutive relation for the deformation of dilatant granular materials. Densification and dilatancy are typical behaviors in cyclic shearing deformation of cohesionless sands under drained conditions. When a water-saturated (drained) sand specimen is subjected to cyclic shearing under a constant effective pressure, deformation-history dependency can be represented by the extreme values of the shear strain and it has a very important influence on the shear stress–strain path and on the material densification. In the course of cyclic shearing, the fabric anisotropy reaches its maximum value at the extreme values of the shear strain. Immediately upon shear reversal, the fabric, the dilatancy parameter, and the overall friction coefficient suffer jumps from their maximum values to their minimum values, as the rate of change of the backstress jumps from its minimum to its maximum value.

A material model that includes shear-deformation-history dependence, describes reasonably well the measured results for the shear strain–stress path and the volumetric deformation. An overall friction coefficient model that includes fabric, void

ratio, and shear-deformation-history dependence gives results in reasonable agreement with the experimental observations.

Acknowledgements

This work has been supported by the National Science Foundation under Grant CMS-9729053, to the University of California, San Diego.

References

Balendran, B., Nemat-Nasser, S., 1993a. Double sliding model for cyclic deformation of granular materials, including dilatancy effects. J. Mech. Phys. Solids 41, 573–612.

Balendran, B., Nemat-Nasser, S., 1993b. Viscoplastic flow of planar granular materials. Mech. Mater. 16, 1–12.

Committee of JSSMFE on the Test Method of Relative Density of Sand, 1979. Maximum-minimum density test method of sand. In: Procedure for Testing Soils, Second Review Edition, JSSMFE, Part 2, pp. 172–188 (in Japanese).

De Josselin de Jong, G., 1971. The double sliding, free rotating model for granular assemblies. Géotechnique 21, 155–163.

Nemat-Nasser, S., 1980. On behavior of granular materials in simple shear. Soils and Foundations 20, 59–73.

Nemat-Nasser, S., 2000. A micromechanically-based constitutive model for frictional deformation of granular materials. J. Mech. Phys. Solids 48, 1541–1563.

Nemat-Nasser, S., Hori, M., 1993. Micromechanics. Elsevier, Amsterdam.

Nemat-Nasser, S., Shokooh, A., 1980. On finite plastic flow of compressible materials with internal friction. Int. J. Solids Struct. 16, 495–514.

Mehrabadi, M.M., Cowin, S.C., 1978. Initial planar deformation of dilatant granular materials. J. Mech. Phys. Solids 26, 269–284.

Oda, M., Konishi, J., Nemat-Nasser, S., 1982. Experimental micromechanical evaluation of strength of granular materials: effects of particle rolling. Mech. Mater. 1, 269–283.

Okada, N., 1992. Energy Dissipation in Inelastic Flow of Cohesionless Granular Media. PhD thesis, University of California, San Diego.

Okada, N., Nemat-Nasser, S., 1994. Energy dissipation in inelastic flow of saturated cohesionless granular media. Géotechnique 44, 1–19.

Rudnicki, J.W., Rice, J.R., 1975. Conditions for the localization of deformation in pressure-sensitive dilatant materials. J. Mech. Phys. Solids 23, 371–394.

Spencer, A.J.M., 1964. A theory of the kinematics of ideal soils under plane strain conditions. J. Mech. Phys. Solids 12, 337–351.

Spencer, A.J.M., 1982. Deformation of ideal granular materials. In: Hopkins, H.G., Sewell, M.J. (Eds.), Mechanics of Solids. Pergamon, Oxford, pp. 607–652.

Spencer, A.J.M., 1986. Instability of steady shear flow of granular materials. Acta Mechanica 64, 77–87.

Subhash, G., Nemat-Nasser, S., Mehrabadi, M.M., Shodja, H.M., 1991. Experimental investigation of fabric-stress relations in granular materials. Mech. Mater. 11, 87–106.